Passive microwave Neural network Precipitation Retrieval (PNPR): an algorithm for cross-track scanning radiometers

Paolo Sanò , Daniele Casella, Stefano Dietrich, Giulia Panegrossi, Marco Petracca, and Alberto Mugnai

Institute of Atmospheric Sciences and Climate (ISAC), Italian National Research Council (CNR)
Area di Ricerca di Tor Vergata, Via del Fosso del Cavaliere 100, 00133, Rome, Italy

Abstract

Within the H-SAF program (Satellite Application Facility on Support to Operational Hydrology and Water Management, http://hsaf.meteoam.it) we have developed a Passive microwave Neural network Precipitation Retrieval algorithm (PNPR) for cross-track scanning radiometers (i.e., MetOp and NOAA AMSU-A/MHS). The main goals of this work have been to obtain a precipitation product optimized for the European area, and to achieve maximum consistency with rain rate estimates from our Cloud Dynamic Radiation Database (CDRD) algorithm, a physically-based Bayesian algorithm developed for conically scanning radiometers (i.e., SSMIS). To achieve this goal we designed and trained the PNPR algorithm using the same physical foundation used for CDRD. To create the training database we carried out 60 simulations over Europe and the Mediterranean area using a cloud-resolving numerical weather prediction model. Then, a Radiative Transfer Modeling System has been used for calculating simulated satellite brightness temperature (TB) vectors consistent with the AMSU-A and MHS channel frequencies, viewing angles, and view-angle dependent IFOV sizes along the scan projections. As opposed to other neural networks (NN) precipitation retrieval algorithms, PNPR uses a unique NN that retrieves the surface precipitation rate for all types of surface backgrounds represented in its database, i.e., land, ocean, ice, snow or coast. This approach prevents different precipitation estimates from being inconsistent with one another when an observed precipitation system extends over two or more types of surfaces. As input data, the PNPR algorithm incorporates the TBs from selected AMSU-A and MHS channels, and various additional TBs-derived variables. In order to reduce the ambiguity, ancillary geophysical inputs (i.e., latitude, terrain height, surface type, season) have been considered during the training phase. PNPR algorithm outputs consist of both the surface precipitation rate and phase. In addition a confidence index is also supplied in order to be able to assess the reliability of the retrieval. The algorithm has also been developed in order to be easily tailored to new cross-track radiometers as they will become available.

1. INTRODUCTION

Neural networks (NNs) are widely applied in an increasing number of meteorological applications for their capability to approximate complex nonlinear and imperfectly known functions. Their main advantage is that they do not need any assumption on the relationship between the input and the output variables. This is due to their ability to learn and generalize, using an adaptive algorithm that minimize the errors between the estimated output and the correct value (the training procedure).

Precipitation is one of the most difficult of all atmospheric variables to retrieve from satellite observations because of the complex and nonlinear relationship between surface precipitation and observed brightness temperatures (TBs). Therefore the use of NNs has been considered in several studies on precipitation analysis based on satellite microwave observations (Chen and Staelin (2003), Surussavadee and Staelin (2008, 2009), Hong et al. (2005)). The Advanced Microwave Sounding Units (AMSU-A and AMSU-B), aboard the U.S. National Oceanic and Atmospheric Administration NOAA-15, NOAA-16, NOAA-18 and NOAA-19 satellites (with the Microwave Humidity Sounder (MHS) replacing AMSU-B on NOAA-18 and NOAA-19 satellites), and aboard the ESA MetOp-A and MetOp-B satellites, are advanced radiometers designed mainly for water vapor and temperature sounding, with a wide use in the retrieval of precipitation. AMSU-A, primarily designed for atmospheric temperature sounding, has 15 channels covering the 50 GHz oxygen band. AMSU-B (and MHS), designed for humidity sounding, has 5 channels near and below the 183 GHz water vapor absorption band. Both

AMSU-A and AMSU-B (or MHS) have a swath of about 2200 km and scan ± 48° from nadir. AMSU-A makes 30 cross-track measurements and has a near nadir instantaneous field of view (IFOV) of 48 km, while AMSU-B makes 90 measurements and has a near nadir IFOV of 16 km. These cross-track scanners provide images with constant angular sampling across track, implying that the IFOV elongates as the beam moves from nadir toward the edge of the scan. The elongation is such that for AMSU-A the IFOV at the edge of the swath is 80 x 150 km^2 and for AMSU-B (and MHS) is 27 x 50 km^2.

The AMSU/MHS channels have a different behavior in the atmosphere. Window channels such as those with frequency bands near 24, 31, 50, 89 and 150 GHz are used for the retrieval of surface precipitation and other surface hydrological products. Opaque channels (bands at 54 and 183 GHz) allow to retrieve temperature and water vapor profiles due to their different sensitivity to specific layers of the atmosphere. In presence of precipitating clouds the temperature/humidity profiling mission fails, because of the presence of hydrometeors and their scattering and absorption processes. The effects of cloud and precipitation on microwave radiances of the AMSU/MHS channels have been extensively analyzed [Burns et al. (1997), Staelin and Chen (2000), Hong et al. (2005), Funatsu et al. (2007)]. Due to the different penetration ability of radiation at microwave frequencies, low-level clouds have little effect on channels near the 183 GHz water vapor band if the sounded atmospheric layers (as characterized by the water-vapor weighting functions) are above the cloud top; on the other hand, high-level clouds lower the TBs due both to the increased absorption by water vapor within the saturated cloud and to the scattering by ice and water droplets (Burns et al., 1997). Moreover, for the three MHS frequencies in the 183 GHz water vapor absorption band, the TB depression increases as the frequency moves away from the center. As a matter of fact, the radiation at 183.31±7 GHz can penetrate deeper into the cloud than for the other two 183 GHz channels and then it is subject to larger scattering from mid and low cloud layers; the 183.31±1 GHz channel primarily responds to deep convection with large, high-density ice particles into the upper atmosphere. These different responses of the three channels, which suggested the possibility to analyze the distribution of different hydrometeors within the cloud can significantly contribute to the estimate of precipitation rates. For example, for convective precipitation the large updraft produces large populations of hydrometeors aloft and can sustain large particles. Thus, a relationship between precipitation rate and updraft velocities and cell top altitudes is to be expected, and, similarly, between precipitation rate and the 183 GHz emission spectrum (Staelin and Chen (2000), Blackwell and Chen (2005)).

The purpose of this paper is to describe the PNPR, a new algorithm for precipitation rate estimation over the European area (25°N to 75°N latitude, 25°W to 45°E longitude), using the different characteristic of AMSU/MHS channels. It is based on a single neural network for all types of background surface (i.e., land, ocean, or coast) trained by a database optimized for the European and Mediterranean basin areas. The algorithm has also been developed in order to be easily adaptable to new cross-track radiometer ATMS on board Suomi NPP satellite. The paper presents a short description of the training database, the process for designing the NN model, the main characteristics of the algorithm and an application to an intense Italian case study over Grosseto region.

2. THE TRAINING DATABASE

The use of neural networks involves a 'training phase' using a large sample of data representative of the input and the output variables used in the retrieval process (in this case AMSU/MHS TBs and surface precipitation rate). The performance of the NN is largely dependent on the completeness and representativeness of the database and on its consistency with the actual observations. In PNPR this dataset is obtained from a cloud-resolving model coupled to a radiative transfer equation model. The database used in this study (fully described in Sanò et al. (2013), Casella et al. (2013), and Smith et al., 2013) includes 60 cloud resolving simulations of different precipitation events over the European area carried out with the University of Wisconsin-Non-Hydrostatic Modeling System (UW-NMS) (Tripoli, 1992), with an advanced microphysics scheme involving 6 different hydrometeor categories. The simulated satellite TB vectors are consistent with the AMSU-A and AMSU-B (MHS) channel frequencies, viewing angles and view-angle dependent IFOV sizes along the scan projections. In essence, the database has been created for the European region, covering the different seasons (15 simulations in each season) and different meteorological situations and precipitation regimes. For

each simulation, three two-way nested grids are configured. The vertical grid extends to 17 km divided into 36 levels with variable, height-dependent grid spacing. The horizontal grid configuration is comprised of: (1) an outer domain of 4,500 x 4,500 km at 50-km resolution, (2) a first interior domain of 900 x 900 km at 10-km resolution, and (3) a second interior and innermost domain of 500 x 500 km at 2-km resolution. Fig. 1 shows the inner domains of the simulations.

In the database, the correspondence between TB vectors, along with their associated surface precipitation rates, is complicated by the dependence of spatial resolution along a radiometer scan due to the varying viewing angle. A variable sensor resolution (VSR) is defined according to the nominal resolution of MHS/AMSU-B, varying from 16 x 16 km^2 / circular at nadir to 26 x 52 km^2 / ovate at scan edge. Thus, the UW-NMS surface precipitation rates were averaged for 45 VSRs. In all, the database contains some 2.5 million profiles for the European / Mediterranean basin region and has 45 views for each entry. See Casella et al. (2013) for an expanded discussion of the cloud profile structure, and database characteristics.

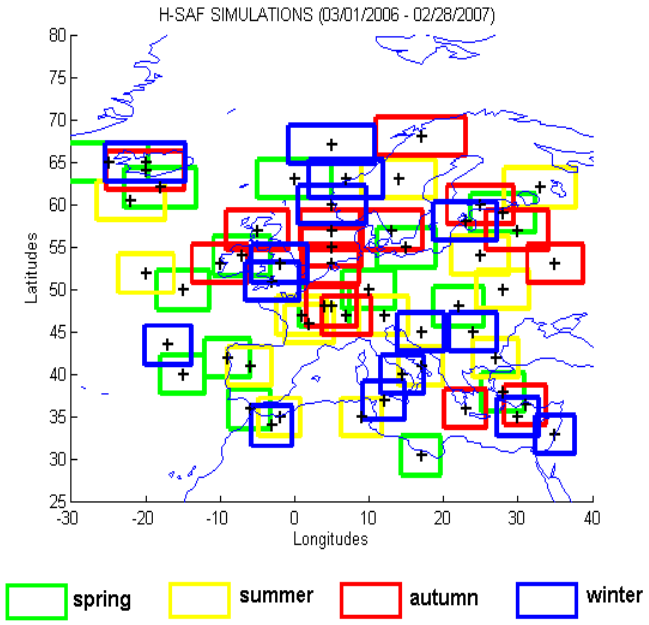

Figure 1: **Inner domains of the 60 NMS simulations, divided by season.**

3. THE NEURAL NETWORK

The architecture of the NN has been carried out using a cross validation method (Anders and Korn, 1999). In the cross validation strategy the comparison between two models is based on the mean square prediction errors (MSPE) which is obtained applying the model to different validation sets. For this purpose a test dataset is used, divided into M subsets containing n observations each. The NN model is repeatedly re-estimated using different dataset of $n(M-1)$ observations, living out a different subset each time. The average MSPE defines the cross validation error. The optimal NN model is obtained comparing the average MSPE of different architectures in a procedure that considers alternately changes in the number of layers, in the number of perceptrons and in the number of inputs.

In the process of defining the architecture of the network, we started considering as input variables all the brightness temperatures of AMSU-A and MHS channels, together with some ancillary data. In particular, in addition to the brightness temperatures, we have considered the following parameters: latitude, longitude, surface altitude, surface classification (land, sea, coast), season, pixel order and secant of the zenith angle of the AMSU/MHS cross-track measurements. Geographical data were introduced in order to reduce the ambiguity in the retrieval. Pixel order and secant of the zenith angle

were needed to determine the degree to which limb smearing is to be considered, an effect produced by the changing atmospheric path length along the scan. The network output is the estimated surface precipitation rate.

Several preliminary analyses have been performed, using the database and experimental data, on the TBs, the ancillary data and other derived parameters, in order to evaluate their contribution to the network performance in estimating the precipitation, and at the same time many different structures of the network have been examined, following the cross validation method. Principal component analysis (PCA) was performed on AMSU-A channels to explore the possibility of reducing the background surface effect (Surussavadee and Staelin, 2008) and improve the network performance. Canonical correlation analysis (CCA) was also carried out to evaluate the strength of the relationships between the TBs and the precipitation. Moreover, the differences of TBs for the 183 GHz channels, Δ_{17}, Δ_{13} and Δ_{37} (corresponding respectively to the differences between channels 183.31±1 and 183.31±7, 183.31±1 and 183.31±3, and 183.31±3 and 183.31±7) have been tested as inputs to the network and their effectiveness in detecting precipitating areas was analyzed [Hong et al. (2005), Funatsu et al. (2007)].

In the process of finding the ANN most suitable for obtaining actual retrievals of surface precipitation rates, the training database is divided into three pieces, the first being used for the actual training (the ground truth piece), the second for providing the synthetic TBs used in a subsequent verification analysis (the ground validation piece), and the third for providing the TBs for the comparison of the different models (the test piece). Notably, all the three pieces need to be representative of all precipitation events contained within the collective database. The choice of size and specific members of each piece are thus crucial in obtaining an effective evaluation of the final ANN's performance. Therefore, for each piece, database members in 45-entry sets from 60 original simulations were selected randomly. During the phase of network design and the training process, more than 200 architectures have been tested and an optimal neural network has been obtained, where "optimal" refers to the best performance of the network (minimum rmse over the full dynamic range of the inputs, and absence of overfitting and of anomalous inhomogeneities in the retrievals).

In order to reduce the complexity of the NN itself, a selection of the input variables with larger effect on the performance of the NN has been carried out. As a result, the following nine inputs have been selected:
1 – A linear combination of TBs in the window channels 50.3, 89, 150 GHz. The coefficients (different for each surface typology) are obtained from the CCA analysis with respect to the surface rain rate. These channels showed the highest correlation coefficients in the CCA analysis in the database.
2 –Δ_{17} difference between the brightness temperatures of channels 183.31±1 and 183.31±7 GHz;
3 - Δ_{37} difference between the brightness temperatures of channels 183.31±3 and 183.31±7 GHz;
4 - Δ_{13} difference between the brightness temperatures of channels 183.31±1 and 183.31±3 GHz;
5 –Type of surface; 6 – Latitude; 7 – Season; 8 – Surface altitude; 9 – Zenith angle.

The feedforward three layers neural network used in this research has 9 input perceptrons, and 20 and 8 perceptrons in the second and third layer (hidden layers) respectively. The tan-sigmoid transfer function is used for the input and the hidden layers and the linear transfer function for the output node. Once the ANN is created, a final check of the retrievals is conducted to determine their stability as the input data vary. To accomplish this, the input TBs are perturbed with random noise within the allowed radiometric errors, followed by associated retrieval calculations. The perturbation retrievals are then compared to those obtained from the original TBs to compute corresponding differences. Since these comparisons did not reveal significant differences, the stability of the optimal ANN was confirmed, enabling its effective implementation within the PNPR algorithm.

4. THE PNPR ALGORITHM

Figure 2 shows the flow diagram of the PNPR algorithm. First, the input TBs undergo a quality check to remove those deriving from occasionally corrupted channels. Moreover, pixels with temperatures less than 50 K or greater than 400 K are discarded and not considered in the retrieval process. A conversion of AMSU-A data to the AMSU-B/MHS grid is performed using a bilinear interpolation. Then, a screening test for identification of potentially precipitating pixels is carried out based on Chen

and Staelin (2003). The 183±7 GHz channel is used for the screening, as it is reasonably good for detecting precipitation also because the angle-dependent variation of precipitation-free brightness temperatures is small when compared to the variation due to precipitation. In the screening procedure the 183±7 GHz TB is compared to a threshold determined empirically, but in very cold and dry atmospheric condition (TB53.6 < 248K) this channel is replaced by the 183±3 GHz with a corresponding new threshold. The input data of potentially precipitating pixels are sent to the network that estimate the corresponding surface precipitation rates. Two additional outputs are estimated by the algorithm, the phase flag and the quality index. The phase flag provides an indication on the phase of the precipitation as listed in Table 1. The determination of the phase flag is based on the studies on snow and ice detection of Surussavadee and Staelin (2009), Rosenkranz (2003), and Kongoli et al. (2003), and with reference to the indices of Grody et al. (2000) for the identification of presence of snowy or iced background.

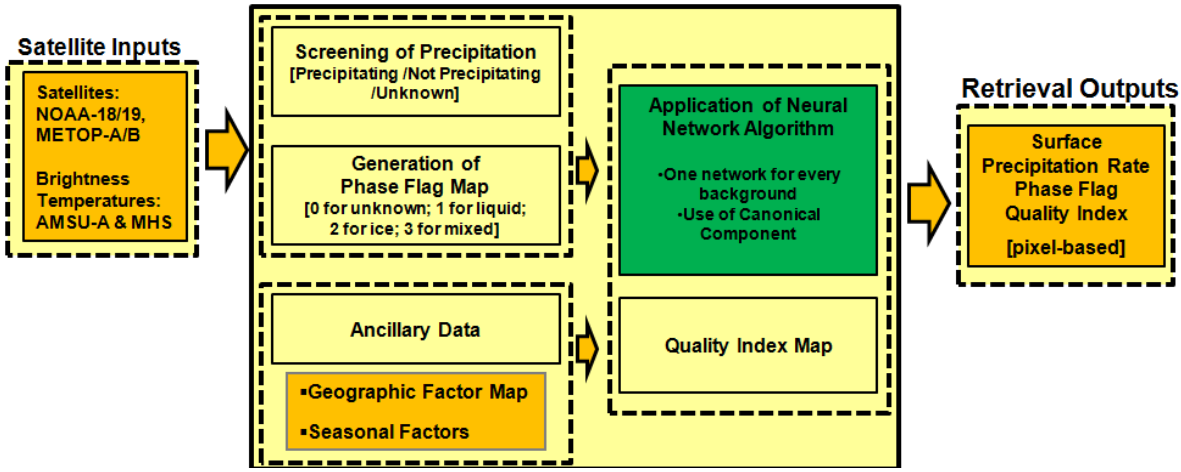

Figure 2: **Block diagram of the PNPR algorithm**

Phase flag	Integer value
unknown (flag determination not reliable)	0
Liquid	1
Ice	2
Mixed	3
missing value (bad data, or precipitation retrieval not available)	7

Table 1**: Phase flag values and interpretation**

The quality index is evaluated on the base of four different criteria:

1. Quality of input data (used sensor, type and number of channels used, horizontal resolution, malfunctioning of radiometers);
2. Background surface index (type of surface, snowy background, presence of ice);
3. Event type index (snow storm, stratiform rain, convective cells);
4. Internal algorithm performance index (i.e., dependence on scan viewing angle).

It allows to identify areas where the retrieval is less or more accurate, and its values range from 0 (0-20 missing data or poor quality) to 100 (80-100 good quality).

The PNPR algorithm is used operationally within the EUMETSAT Hydrology Satellite Application Facility (H-SAF) to generate surface precipitation rate (with indication of phase) from cross-track scanning radiometers [H-SAF product H02 (ver. 2.4), available at http://hsaf.meteoam.it]. Please, refer to Mugnai et al. (2013a, b) for an overview of the H-SAF project and a full description of all the H-SAF precipitation products.

5. THE CASE STUDY

An intense Italian case study over Grosseto region is analyzed in this section. The Grosseto flood occurred in the period between 11 and 12 November 2012. The event has been analyzed considering all the available satellite overpasses on the Grosseto area: six overpasses on 11 November, 2012 (NOAA-19 01:26 and 12:53 UTC, NOAA-18 02:09 and 13:56 UTC, MetOp-A 09:34 and 19:26 UTC) and five overpasses on 12 November, 2012 (NOAA-19 01:15 and 12:42 UTC, NOAA-18 01:58 and 13:25 UTC, MetOp-A 09:23 UTC). Italian rain gauge network measured an accumulated precipitation of about 327 mm/24 h during the most intense phase. Figure 3 shows the PNPR input variables derived from the NOAA-18 AMSU-A/MHS overpass at 13:25 UTC on 12 November, 2012. In the top panels (from left to right) the result of the CCA (obtained using the TBs of 50, 89 and 150 GHz channels) and the Δ_{17} difference. The bottom panels present (from left to right) the Δ_{37} and Δ_{13} differences. It is evident in the four panels the clear identification of heavy precipitation areas, and the ability of these derived variables to screen out the background surface effects.
Figure 4 shows in the first row (from left to right) the surface rain rate map (mm/h) produced by the PNPR algorithm, and the associated quality index. The surface rain rate is ranging from 10 mm/h to 15 mm/h in the area affected by the flood and the corresponding quality index is around 80 (good quality). The estimated precipitation phase is presented in the bottom panel. The precipitation estimates obtained for the different overpasses were in good agreement with the hourly raingauge measurements available for the event, averaged at the horizontal resolution of the PNPR.

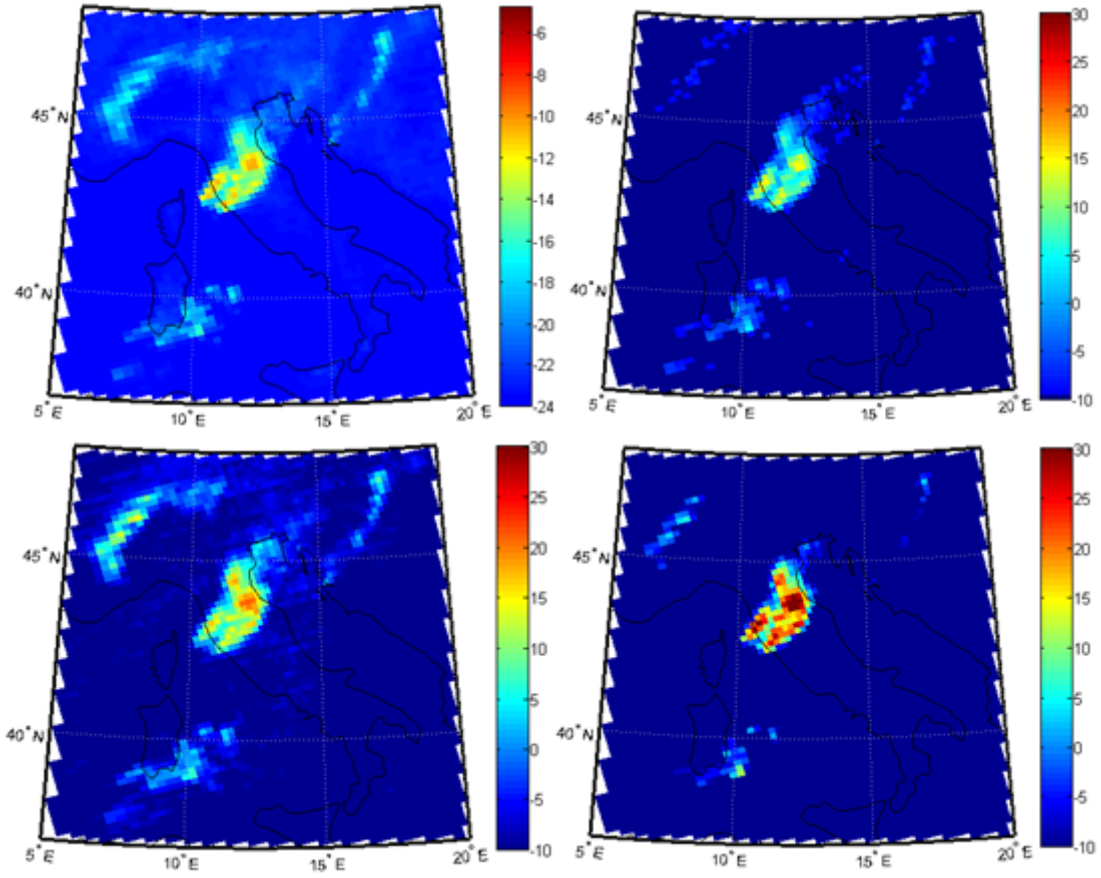

***Figure 3*: Grosseto flood (11 and 12 November 2012). The top panels show (from left to right) the CCA (obtained using the TBs of 50, 89 and 150 GHz channels, for the selected overpass of NOAA-18 AMSU-A/MHS at 13:25 UTC on 12 November, 2012) and the Δ_{17} difference. The bottom panels show the Δ_{37} (left) and Δ_{13} (right) differences.**

The performance of the PNPR algorithm has been tested and verified on 20 different precipitation systems in Europe by comparing the retrievals with the ground-based radar and raingauge data made available by the H-SAF Precipitation Product Ground Validation team. The results of this study, showing the good performance of the PNPR algorithm and comparisons with to the previous version of the H-SAF H02 product are presented and discussed in Panegrossi et al. (2013, this issue). In this study, The PNPR estimates are compared to those obtained from the CDRD algorithm (H-SAF

operational product H01 Ver. 1.7) to verify the consistency of the retrievals from close-in-time overpasses of cross-track (AMSU/MHS) and conically scanning (SSMIS) radiometers (Casella et al. (2013), Sanò et al. (2013)).

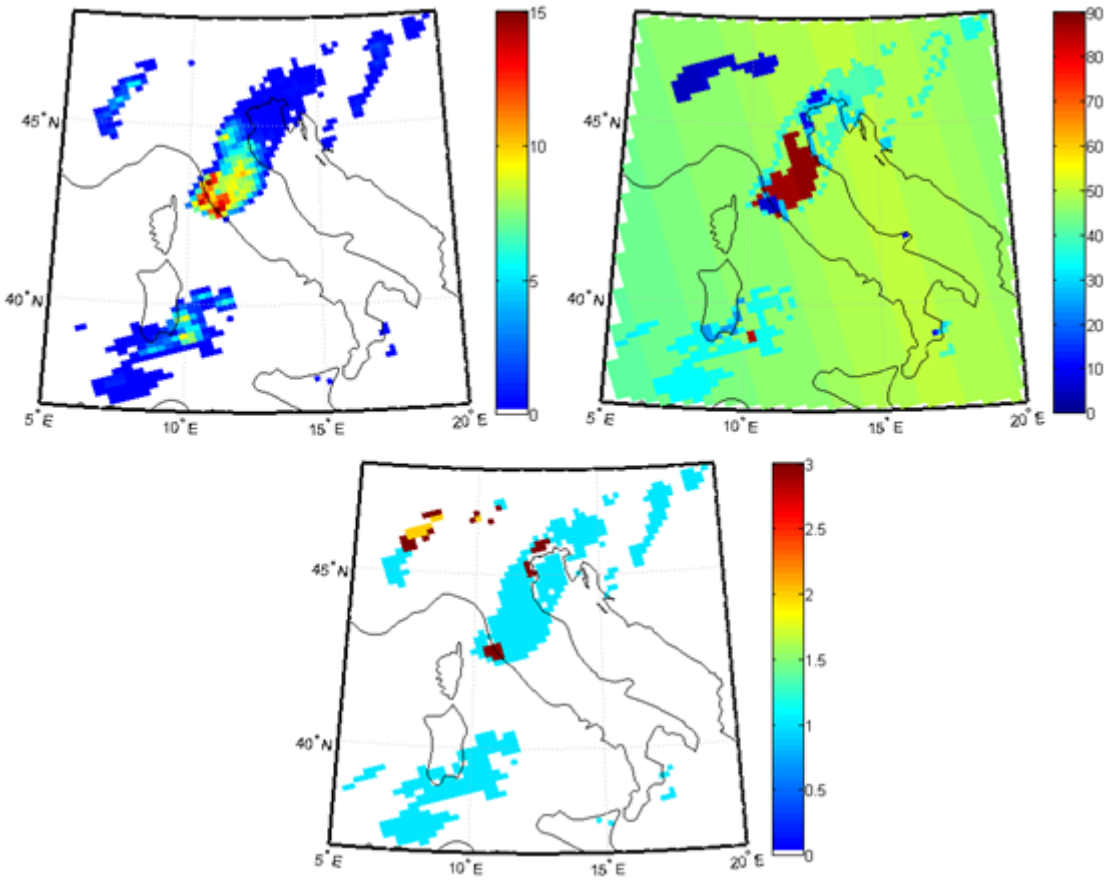

Figure 4: **Grosseto flood (11 and 12 November 2012). In the top panels (from left to right)) the surface rain rate map (mm/h) produced by the PNPR algorithm and the associated quality index are shown. The bottom panel presents the precipitation phase (see Table 1).**

5. CONCLUSIONS

The purpose of this paper was to describe the new PNPR algorithm designed for precipitation rate estimation over the European and the Mediterranean basin area, using AMSU/MHS measurements, based on a single neural network for different background surfaces (land, coast and ocean), trained using training dataset built from cloud-radiation model simulations. The results obtained in the application of the PNPR algorithm under different meteorological conditions in Europe (storm producing flood, convective events, moderate/light precipitation) have shown good potentials of the algorithm in the identification of precipitating systems, and in precipitation retrieval accuracy over different surface types. The neural network is currently being used as a deliverable within the EUMETSAT H-SAF project, for producing operational satellite-based surface precipitation rates from cross-track scanning radiometers. Extension of the algorithm to the MSG full-disk area (Africa and Southern Atlantic) is under development. Moreover, a training dataset to be used for the ATMS on board the Suomi NPP satellite has been developed and preliminary studies aimed at evaluating the benefits from the availability of ATMS data are being carried out.

REFERENCES

Anders U., O. Korn, 1999, Model selection in neural networks, Neural Networks, vol. 12, pp. 309-323.

Blackwell W.J., F. W .Chen, 2005, Neural Network Applications in High-Resolution Atmospheric Remote Sensing, Lincoln Laboratory Journal, vol. 15, n. 2, pp. 299-322.

Burns B. A., X. Wu, G. R. Diak, 1997, Effects of precipitation and cloud ice on brightness temperatures in AMSU moisture channels, IEEE Trans. Geosci. Remote Sens., vol. 35, 6, pp. 1429–1437.

Casella D., S. Dietrich, M. Formenton, A. Mugnai, G. Panegrossi, P. Sanò, E. A. Smith, and G. J. Tripoli, 2012, Verification of Cloud Dynamics and Radiation Database (CDRD) passive microwave precipitation retrieval algorithm using TRMM satellite radar and radiometer measurements over Southern Mediterranean Basin, in Microwave Radiometry and Remote Sensing of the Environment (MicroRad), 2012 12th Specialist Meeting, pp. 1-4.

Casella D., G. Panegrossi, P. Sanò, A. Mugnai, E. A. Smith, G.J. Tripoli, S. Dietrich, M. Formenton, W.Y. Leung, A. Mehta, 2013, Transitioning from CRD to CDRD in Bayesian Retrieval of Rainfall from Satellite Passive Microwave Measurements: Part 2. Overcoming Database Profile Selection Ambiguity by Consideration of Meteorological Control on Microphysics. IEEE Trans. Geosci. Remote Sens., vol.51, no.9, pp.4650,4671.

Chen F.W., D.H. Staelin, 2003, AIRS/AMSU/HSB precipitation estimates, IEEE Trans. Geosci. Remote Sens., vol. 41, issue 2, pp. 410 – 417.

Funatsu B.M., C. Claud, J.-P. Chaboureau, 2007, Potential of Advanced Microwave Sounding Unit to identify precipitating systems and associated upper-level features in the Mediterranean region: Case studies, J. Geophys. Res.,vol. 112, D17113, 19 pp.

Grody N., F. Weng, R. Ferraro, 2000, Application of AMSU for obtaining hydrological parameters, Microwave Radiometry and Remote Sensing of the Earth's Surface and Atmosphere, P. Pampaloni, S. Paloscia, eds., VSP, pp.339-352.

Hong G., G. Heygster, J. Miao, K. Kunzl, 2005, Detection of tropical deep convective clouds from AMSU-B vater vapor channels measurements, J. Geophys. Res., vol. 110, pp. 15.

Kongoli C., P. Pellegrino, R. R. Ferraro, N. C. Grody, H. Meng, 2003, A new snowfall detection algorithm over land using measurements from the Advanced Microwave Sounding Unit (AMSU), Geophysical Research Letters, vol. 30, n. 14, L1756, 4 pp.

Mugnai A., E. A. Smith, G. J. Tripoli, B. Bizzarri, D. Casella, S. Dietrich, F. Di Paola, G. Panegrossi, P. Sanò, 2013a, CDRD and PNPR Satellite Passive Microwave Precipitation Retrieval Algorithms: EuroTRMM / EURAINSAT Origins and H-SAF Operations, Nat. Hazards Earth Syst. Sci, 13, 887–912

Mugnai A., D. Casella, E. Cattani, S. Dietrich, S. Laviola, V. Levizzani, G. Panegrossi, M. Petracca, P. Sanò, F. Di Paola, D. Biron, L. De Leonibus, D. Melfi, P. Rosci, A. Vocino, F. Zauli, S. Puca, A. Rinollo, L. Milani, F. Porcù, and F. Gattari, 2013b, Precipitation Products from the Hydrology SAF, Nat. Hazards Earth Syst. Sci, 13, 1959-1981

Panegrossi G., D. Casella, S. Dietrich, P. Sanò, M. Petracca, A. Mugnai, 2013, A Vaerification study over Europe of AMSU/MHS and SSMIS passive microwave precipitation retrieval, Proc. 2013 Joint EUMETSAT/AMS Meteorological Satellite Conference.

Rosenkranz P.W., 2003, Rapid Radiative Transfer Model for AMSU/HSB Channels, IEEE Trans. Geosci. Remote Sens., vol 41, n.2, February 2003, pp.362-368.

Sanò P., D. Casella, A. Mugnai, G. Schiavon, E.A. Smith, G.J. Tripoli, 2013, Transitioning from CRD to CDRD in Bayesian Retrieval of Rainfall from Satellite Passive Microwave Measurements: Part 1. Algorithm Description and Testing, IEEE Trans. Geosci. Remote Sens., vol. 51, no. 7, 4119-4143,

Smith E.A., H. W.-Y. Leung, J.B. Elsner, A.V. Mehta, G.J. Tripoli, D. Casella, S. Dietrich, A. Mugnai, G. Panegrossi and P. Sanò, 2013, Transitioning from CRD to CDRD in Bayesian Retrieval of Rainfall from Satellite Passive Microwave Measurements: Part 3. Identification of Optimal Meteorological Tags, Nat. Hazards Earth Syst. Sci, 13, 1185–1208.

Staelin D.H., F. W. Chen, 2000, Precipitation observations near 54 and 183 GHz using the NOAA-15 satellite, IEEE Trans. Geosci. Remote Sens., vol. 38 , 5, Part 1, pp. 2322 – 2332.

Surussavadee C., D. H. Staelin, 2008, Global Millimeter-Wave Precipitation Retrievals Trained With a Cloud-Resolving Numerical Weather Prediction Model, Part I: Retrieval Design, IEEE Trans. Geosci. Remote Sens., vol 46, n.1, pp.99-108.

Surussavadee C., D. H. Staelin, 2009, Satellite Retrievals of Artic and Equatorial Rain and Snowfall Rates Using Millimeter Wavelengths, IEEE Trans. Geosci. Remote Sens., vol 47, n.11, pp.3697-3707.

Tripoli G.J., A nonhydrostatic mesoscale model designed to simulate scale interaction, Mon. Weather Rev., vol. 120, no. 7, pp. 1342–1359, Jul. 1992.